PNAS RESEARCH ARTICLE | IMMUNOLOGY AND INFLAMMATION OPEN ACCESS

PD-1 blockade following ART interruption enhances control of pathogenic SIV in rhesus macaques

Vijayakumar Velu[a,b,1], Kehmia Titanji[a], Hasan Ahmed[a], Ravi Dyavar Shetty[a], Lakshmi S. Chennareddi[a,c], Gordon J. Freeman[d,e], Rafi Ahmed[a,c], and Rama Rao Amara[a,c,1]

Edited by Malcolm Martin, National Institute of Allergy and Infectious Diseases, Bethesda, MD; received February 5, 2022; accepted July 11, 2022

Programmed death-1 (PD-1) blockade during chronic Simian immunodeficiency virus (SIV) infection results in restoration of CD8 T-cell function and enhances viral control. Here, we tested the therapeutic benefits of PD-1 blockade administered soon after anti-retrovial therapy (ART) interruption (ATI) by treating SIV-infected and ART-suppressed macaques with either an anti-PD-1 antibody ($n = 7$) or saline ($n = 4$) at 4 wk after ATI. Following ATI, the plasma viremia increased rapidly in all animals, and the frequency of SIV-specific CD8 T cells also increased in some animals. PD-1 blockade post ATI resulted in higher proliferation of total memory CD8 and CD4 T cells and natural killer cells. PD-1 blockade also resulted in higher proliferation of SIV-specific CD8 T cells and promoted their differentiation toward better functional quality. Importantly, four out of the seven anti-PD-1 antibody-treated animals showed a rapid decline in plasma viremia by 100- to 2300-fold and this was observed only in animals that showed measurable SIV-specific CD8 T cells post PD-1 blockade. These results demonstrate that PD-1 blockade following ATI can significantly improve the function of anti-viral CD8 T cells and enhance viral control and strongly suggests its potential synergy with other immunotherapies that induce functional CD8 T-cell response under ART. These results have important implications for HIV cure research.

PD-1 | SIV | HIV | HIV cure

Significance

Anti-viral CD8 T cells express high levels of the co-inhibitory receptor programmed death-1 (PD-1) during chronic HIV and Simian immunodeficiency virus (SIV) infections and in vivo PD-1 blockade during chronic SIV infection restores CD8 T-cell function and improves viral control. However, it is important to define at what stage of chronic infection PD-1 blockade provides the most therapeutic benefit. In this report, we show a short-term PD-1 blockade administered 4 weeks after anti-retroviral therapy interruption provides substantial therapeutic benefit by improving the function of anti-viral CD8 T-cell immunity and rapidly controlling viremia.

Anti-viral CD8 T cells during chronic viral infections such as lymphocytic choriomeningitis virus (LCMV), HIV, and Simian immunodeficiency virus (SIV) maintain high levels of PD-1 expression that is associated with their impaired polyfunctionality and proliferation (1–5). High levels of PD-1 expression on HIV-specific CD4 and CD8 T cells correlated positively with high viral load, faster disease progression, and the blockade of PD-1 in vitro-enhanced T-cell function (2–4). Initial studies in chronically infected LCMV clone 13-infected mice showed exhaustion of antigen-specific T cells can be successfully reversed after PD-1 blockade in vivo leading to reduced viral levels (5). Similarly, we and others demonstrated that in vivo blockade of PD-1 in chronically SIV-infected rhesus macaques (RMs) enhance the function of anti-viral CD8 T cells and B cells, leading to reduced plasma viral set points and hyperimmune activation (1, 6, 7). More recently, we demonstrated that PD-1 blockade during anti-retroviral therapy (ART) with and without therapeutic vaccination reduces viral reservoirs and plasma viral set point post ART interruption (8, 9). Thus, augmenting cellular immunity by targeting the PD-1 pathway is of significant interest to HIV cure research, as anti-viral CD8 T cells are critical for controlling HIV replication early after primary infection (10–12) and under suppressive ART (13, 14). Although in vivo PD-1 blockade has been tested either during chronic infection or during ART therapy in SIV-infected macaques, it is not known whether PD-1 blockade following ART interruption (ATI) has any effects on restoring/enhancing anti-viral immune function and improving viral control in SIV-infected RMs. In the current study, we hypothesized that the therapeutic benefits of PD-1 blockade can be improved further to enhance control of reemerging viremia when administered soon after ATI. Hence, we evaluated the effects of PD-1 blockade administered 4 wk after ATI in chronically SIV-infected RMs. We chose 4 wk after ATI to allow for viral rebound to its peak and to monitor for recall of SIV-specific CD8 T cells post ATI. This information would allow us to study the impact of PD-1 blockade on viral control and the contribution of CD8 T cells.

Results and Discussion

A total of 11 rhesus macaques were enrolled in the study and were infected intravenously with SIVmac251. At week 16 post SIV infection, all animals received ART for 21 wk, after which the treatment was interrupted. Animals were randomized into two

Author contributions: V.V., R.R.A., and R.A. designed research; V.V., K.T., H.A., and R.D.S. performed research; G.J.F. contributed new reagents/analytic tools; V.V., K.T., H.A., R.D.S., L.S.C., and R.A. analyzed data; and V.V. and R.A. wrote the paper.

Competing interest statement: V.V., K.T., G.J.F., R.A., and R.R.A. are co-inventors of PD-1 technology that has been licensed to Genentech by Emory University. GJF has patents/pending royalties on the PD-1/PD-L1 pathway from Roche, Merck MSD, Bristol-Myers-Squibb, Merck KGA, Boehringer-Ingelheim, AstraZeneca, Dako, Leica, Mayo Clinic, and Novartis. GJF has served on advisory boards for Roche, Bristol-Myers-Squibb, Xios, Origimed, Triursus, iTeos, NextPoint, IgM, Jubilant and GV20. GJF has equity in Nextpoint, Triursus, Xios, iTeos, IgM, and GV20.

This article is a PNAS Direct Submission.

[1]To whom correspondence may be addressed. Email: ramara@emory.edu or vvelu@emory.edu.

This article contains supporting information online at http://www.pnas.org/lookup/suppl/doi:10.1073/pnas.2202148119/-/DCSupplemental.

Published August 8, 2022.

groups (Fig. 1*A*). The PD-1 group ($n = 7$) received six doses of humanized anti-PD-1 antibody (3 mg/kg) on days 0, 3, 7, 14, 21, and 28 starting from 4 wk post ATI. The control group ($n = 4$) received normal saline. Animals were randomized into these two groups based on the viral set point, the magnitude of SIV-specific interferon (IFN)γ^+ CD8 T cells and level of PD-1 expression on total and SIV-specific CD8 T cells at the time of ART initiation (*SI Appendix*, Fig. 1 *A–E*). Four out of seven animals in the PD-1 group and two out of four animals in the control group expressed the Mamu-A01 allele, which enabled us to detect SIV-specific Gag-CM9$^+$ CD8 T-cell response using Gag-CM9 tetramer. All macaques were monitored for the immunological and virologic measurements post-ATI and after PD-1 blockade. Two animals in each group did not show complete viral suppression. The virus rebounded rapidly in all animals by 4 wk post ATI. The frequency of IFNγ^+ SIV-specific CD8 T cells declined by approximately tenfold following ART, expanded by 4 wk after ATI in some animals and were comparable between the two groups at the time of PD-1 blockade (*SI Appendix*, Fig. 1 *C* and *D*). The level of exhaustion marker PD-1 expression on total and SIV-specific CD8 T cells also declined in both groups following ART ($P = 0.03$) and did not increase significantly at 4 wk after ATI, the time of PD-1 blockade, suggesting that animals randomized for PD-1 infusion were not different from the control animals in terms of their virological and immunological parameters before infusing the PD-1 antibody.

Following administration of anti-PD-1 antibody at 4 wk post-ATI, we observed a significant increase in the proliferation of circulating total CD8$^+$ and CD4$^+$ T cells as measured by

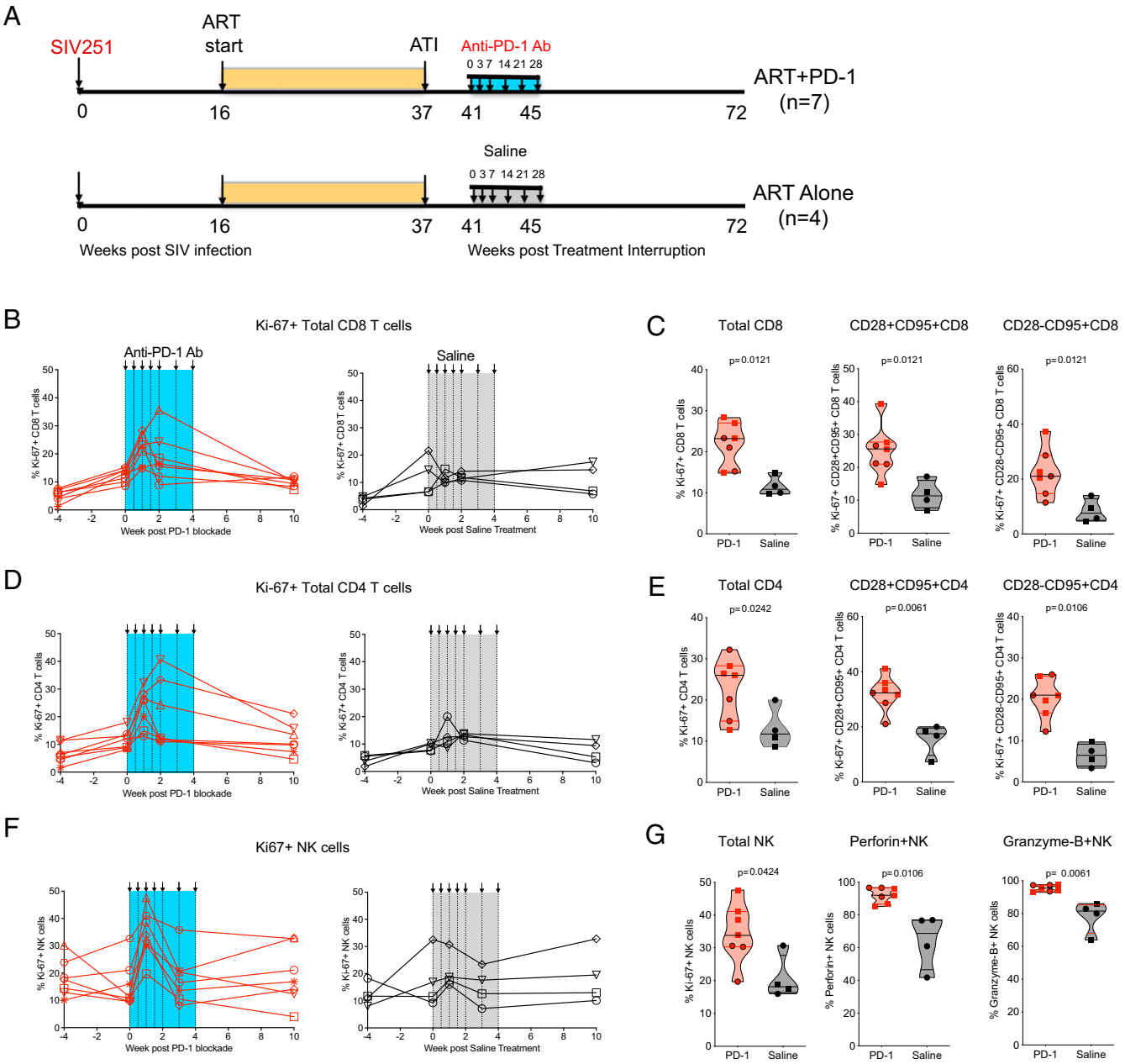

Fig. 1. PD-1 blockade post ATI enhances proliferation of CD8 T, CD4 T, and NK cells in the blood. (*A*) Schematic of monkey study design. (*B* and *D*) Temporal frequency of proliferating (K_i-67$^+$) total CD8 (*B*) or CD4 (*D*) T cells post PD-1 blockade. (*C* and *E*) Frequency of K_i-67$^+$ total, central memory (CD28$^+$CD95$^+$), effector memory (CD28$^-$CD95$^+$) CD8 (*C*), or CD4 (*E*) T cells at day 7 post PD-1 blockade. (*F*) Temporal frequency of proliferating NK cells. (*G*) Frequency of perforin$^+$ and granzyme-B$^+$ NK cells at day 7 post PD-1 blockade. The Mamu-A*01$^+$ animals are identified with square symbol in (*C*), (*G*), and (*E*).

K_i-67 expression that peaked around day 7 post PD-1 blockade for both $CD8^+$ and $CD4^+$ T cells (Fig. 1 *B*–*E*). Similarly, both central memory ($CD28^+CD95^+$, TCM) and effector memory ($CD28^-CD95^+$, TEM) $CD8^+$ and $CD4^+$ T cells showed significant induction of K_i-67 and all peaked by day 7 post-PD-1 blockade. In addition to T cells, we also observed a significant increase in the proliferation of natural killer (NK) cells in the PD-1 treated animals at day 7 post-PD-1 blockade (Fig. 1*F*). The frequency of perforin$^+$ or granzyme B^+ NK cells was also higher at day 7 post PD-1 blockade (Fig. 1*G*). These results showed that PD-1 blockade following ATI markedly enhanced the proliferative potential of $CD8^+$ T cells, $CD4^+$ T cells, and NK cells.

We next looked at the expansion of SIV-specific $CD8^+$ T cells post PD-1 blockade. We monitored the kinetics and the functional phenotype of Gag-CM9 specific-CD8 T cells in Mamu-$A*01^+$ animals post PD-1 blockade (Fig. 2). The frequency of Gag-CM9 tetramer$^+$ CD8 T cells increased significantly from the day of ATI to week 4 ATI in all animals and ranged from 1.6 to 7% (Fig. 2 *A* and *B*). In the two control animals, the frequency of these cells either further increased or stayed constant after week 4 post ATI. However, we observed a different pattern for the frequency of Gag-$CM9^+$ CD8 T cells in the PD-1 group. One animal showed an expansion, two animals did not show an expansion, and one animal showed a decline after PD-1 blockade. The lack of expansion or decline of Gag-$CM9^+$ CD8 T cells was observed despite an increase in K_i-67 expression on these cells at day 7 post PD-1 blockade (Fig. 2*C*). At this point, it is not clear what mechanisms contributed to this. We then looked at the functional quality of Gag-CM9 tetramer$^+$ cells between the two groups by comparing the frequency of Gag-CM9 tetramer-specific CD8 T cells that coexpressed CD28 (costimulation potential), CD127 (proliferative potential), and CCR7 (lymph-node homing potential, memory marker). We observed a significant increase for the coexpression of CD28 ($P = 0.02$) (Fig. 2*D*), CCR7 ($P = 0.007$) (Fig. 2*E*), and CD127 ($P = 0.02$) (Fig. 2*F*) by 4 wk after the PD-1 blockade in the PD-1 blockade group compared to the control group animals. The expression of these markers either stayed constant or further increased in the PD-1 group over 30 wk. In contrast, the Gag-CM9 tetramer$^+$ cells in the control group showed a gradual decline. The higher CD28 expression is indicative of better costimulatory response potential of these anti-viral CD8 T cells. The higher CCR7 expression indicates more preferential migration of anti-viral CD8 T cells to lymph nodes where large fraction of viral reservoirs persist. Overall, these results demonstrated that in vivo blockade of PD-1 soon after the ATI either preserved or enhanced the functional phenotype of SIV-specific CD8 T cells long after discontinuation of anti-PD-1 antibody treatment.

We next looked at the cytokine production capacity of SIV-specific CD8 T cells to see whether PD-1 blockade improved the T-cell function. For Mamu-$A*01^+$ animals, we stimulated total PBMC with Gag-CM9 peptide and looked for the production of IFN-γ and calculated the percentage of IFNγ^+ cells of total Gag-CM9 tetramer$^+$ cells for each animal following PD-1 blockade. A higher percentage would indicate better function. An example of comparison between Gag-CM9 tetramer$^+$ CD8 T cells and Gag-CM9 peptide-stimulated IFN-γ^+ CD8 T cells at week 0 and week 6 post PD-1 blockade for PD-1-treated and control group animals is shown in Fig. 3*A*. The functional capacity of Gag-CM9 CD8 T cells increased by day 7 in PD-1-treated animals and this was not observed in the control animals (Fig. 3*B*). At day 7, the PD-1-treated animals showed a higher percentage of functional CD8 T cells compared to controls (Fig. 3*C*). We next measured the total Gag-specific IFN-γ^+ (Fig. 3 *D* and *F*) and IFN-γ^+ tumor necrosis factor (TNF)α^+ (Fig. 3 *E* and *G*) CD8 and CD4 T cells by stimulating with Gag-peptide pool at multiple time points following ATI and PD-1 blockade. As expected, we observed an increase for cytokine$^+$ CD8 and CD4 T cells between week 0 and week 4 post ATI in both groups and there was a considerable variability between animals in each group. Following PD-1 blockade, the frequency of cytokine$^+$ cells either increased or stayed relatively constant in some animals. However, there was no significant difference between the two groups. It is important to note that T-cell expansion post ATI is influenced by the viral burden, and generally higher virus replication drives higher T-cell expansion. Thus, it was hard to compare the magnitude of cytokine$^+$ T cells between the two groups since we saw better viral control in the PD-1 treated group (see below).

To understand the therapeutic benefit of the PD-1 blockade, we assessed the kinetics of viral RNA levels in plasma until approximately 7 mo post ATI (30 wk). Following ATI, the plasma viremia increased rapidly in all animals by 4 wk as discussed above. Interestingly, the PD-1 blockade at 4 wk post ATI resulted in a mixed virologic response. Some animals responded well and virus levels declined (solid lines, responders) and some animals did not (dotted lines, nonresponders). During this phase, the saline-treated control animals did not show any sign of viral control (solid black line) (Fig. 4*A*). Four out of the seven animals treated with PD-1blockade showed a decline (100- to 2500-fold) in viral load, and the decline was transient and persisted up to 4 wk post PD-1 blockade. This was presumably due to rapid development of anti-drug antibodies that resulted in clearance of anti-PD-1 antibody by day 21 post PD-1 blockade (*SI Appendix*, Fig. 2). Of the four responders, three were Mamu-$A*01^+$ and one was Mamu-$A*01^-$. Three out of seven animals failed to show any virologic benefit following PD-1 blockade. Of the three nonresponders, one was Mamu-$A*01^+$ and two were Mamu-$A*01^-$. These results suggested that virologic benefit of PD-1 blockade could be better in the Mamu-$A*01^+$ animals compared to Mamu-$A*01^-$ animals. This is anticipated given that the magnitude of SIV Gag-specific CD8 T-cell response is generally greater in the Mamu-$A*01^+$ animals compared to Mamu-$A*01^-$ animals due to immunodominance of the Gag-CM9 epitope. The PD-1 group animals showed significantly lower viremia at the dip (lowest viral load between weeks 4–8 post ATI) post PD-1 blockade and this was not observed in the control animals (Fig. 4*B*). Although there was a mixed virologic response, when we compared the set-point viral load pre-ART and post ATI we observed a significant reduction ($P = 0.002$) in the PD-1 group but not in the control group (Fig. 4*C*). The frequency of peak SIV Gag-specific CD8 T cells post PD-1 blockade showed a strong association with enhanced viral control post PD-1 blockade as evidenced by the inverse correlation with the level of viremia at the dip post PD-1 blockade in the PD-1 group (Fig. 4*D*). In contrast, no association was observed in the control group. These data suggested an important role for anti-viral CD8 T cells in viral control post PD-1 blockade.

In conclusion, our results demonstrated that in vivo blockade of PD-1 early post ATI in chronically SIV-infected animals results in rapid expansion of central and effector memory CD8 and CD4 T cells and cytolytic NK cells in the blood. Importantly, PD-1 blockade also improved the functional quality of SIV-specific CD8 T cells and rapidly controlled the reemerging viremia. As discussed above, the virologic benefits of PD-1

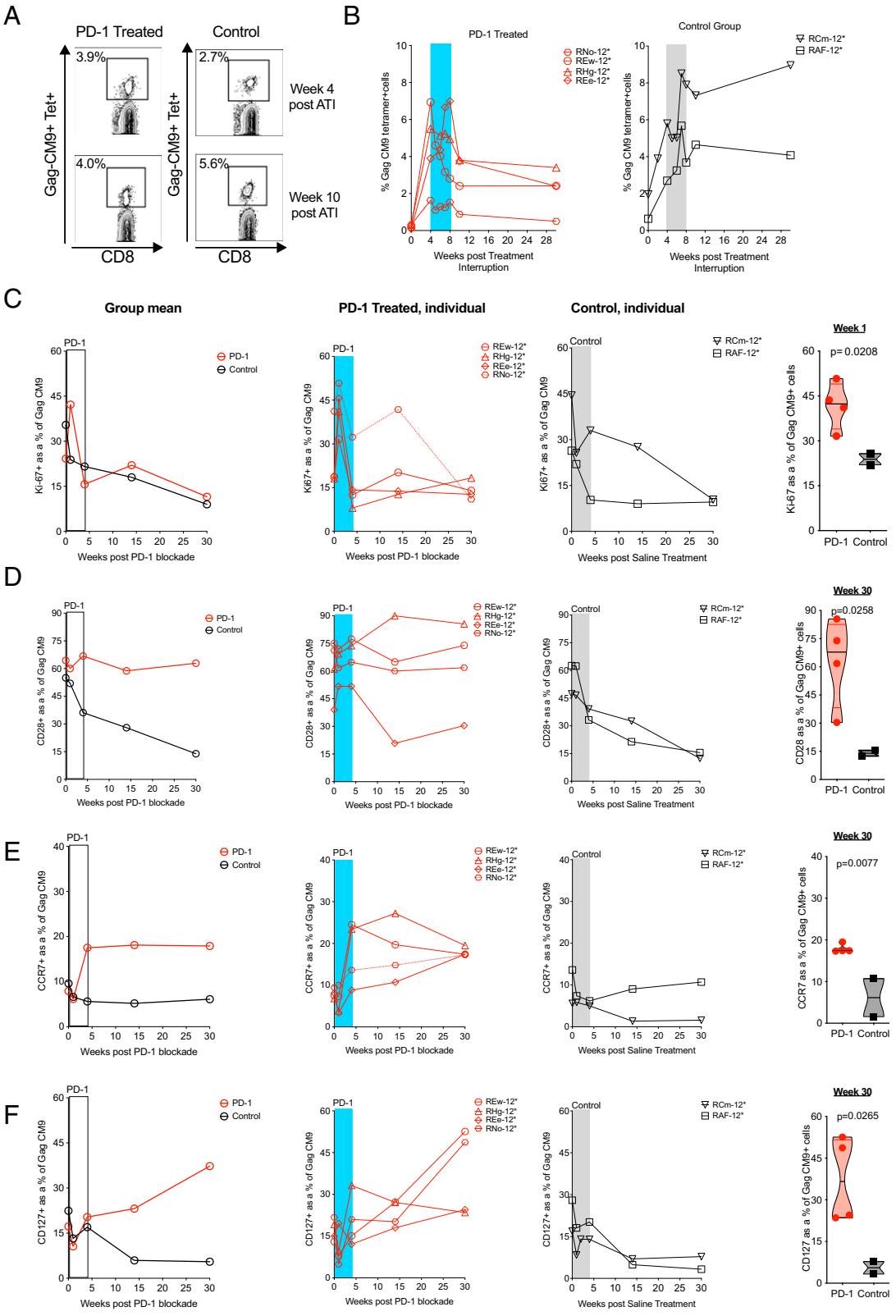

Fig. 2. PD-1 blockade post ATI enhances the functional phenotype of SIV-Gag-CM9^{+} CD8 T cells in blood. (*A*) Representative fluorescence-activated cell sorter (FACS) plots showing the Gag-CM9 tetramer^{+} CD8 T cells. Numbers on the FACS plots represent the frequency of tetramer^{+} cells as a percent of total CD8 T cells. (*B*) Temporal frequency of Gag-CM9 tetramer^{+} CD8 T cells post ATI in anti-PD-1 Ab treated (n = 4 Mamu-A*01^{+}) and control (n = 2 Mamu-A*01^{+}) animals. (*C*–*F*) Frequency of tetramer^{+} cells coexpressing K_i-67 (*C*), CD28 (*D*), CCR7 (*E*), and CD127 (*F*) following PD-1 blockade.

blockade were transient presumably due to rapid clearance of humanized anti-PD-1 antibody used in this study. The persistence of anti-PD-1 antibody can be improved by using a primatized anti-PD-1 antibody that will reduce the generation of anti-drug antibody response and may provide longer lasting virologic benefits. Our results also demonstrated that animals that generated stronger anti-viral CD8 T-cell response following PD-1 blockade are likely to show better viral control.

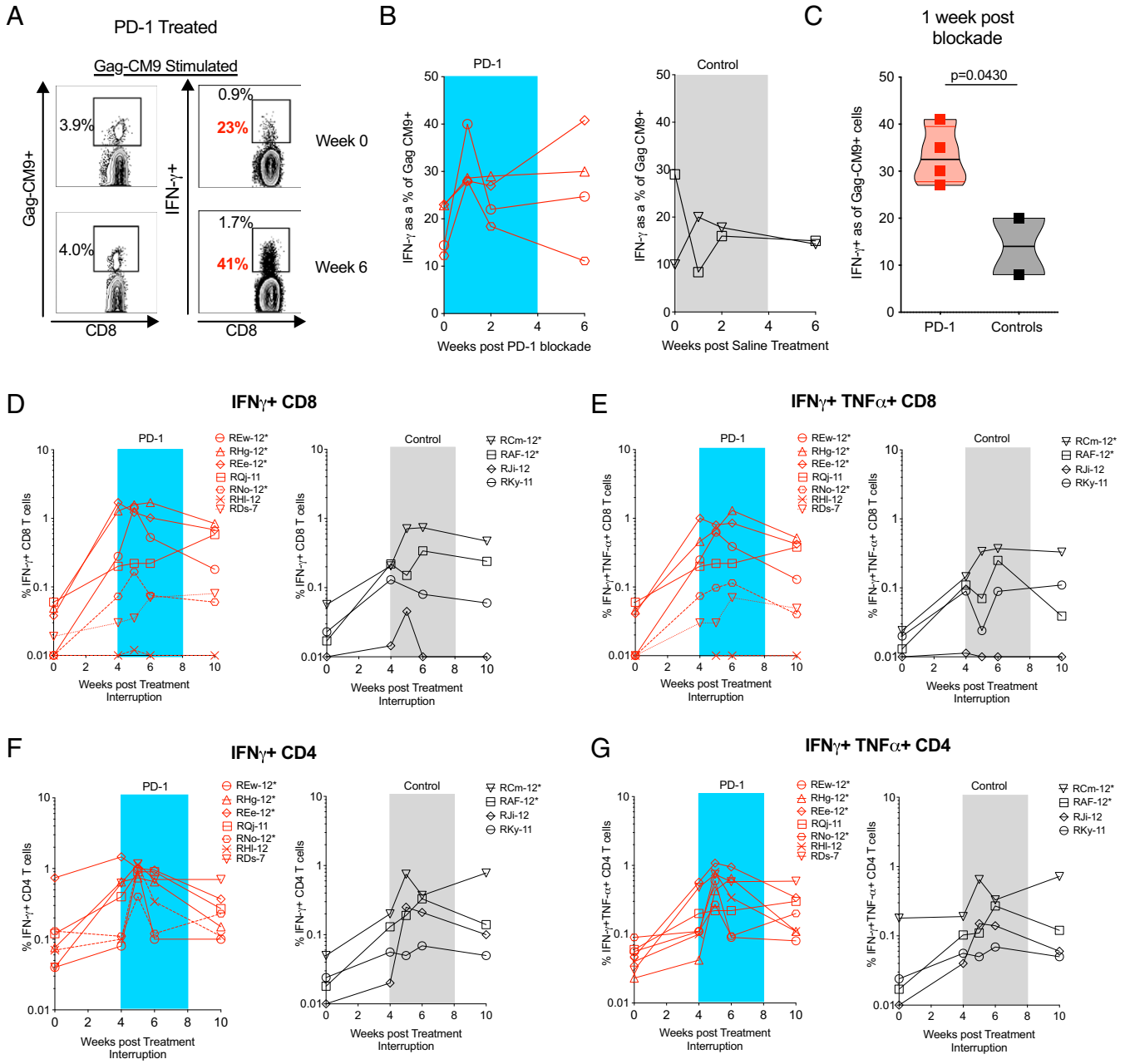

Fig. 3. PD-1 blockade after ATI improved cytokine producing function of SIV-specific CD8 T cells. (*A*) Representative flow plots showing the frequency of Gag-CM9 tetramer$^+$ cells and IFN-γ^+ CD8 T cells following stimulation with Gag-CM9 peptide. Numbers with bold red font on the FACS plots represent the percent of IFN-γ^+ producing cells as a percent of tetramer$^+$ cells. (*B*) Percent of IFN-γ^+ producing cells as a percent of tetramer$^+$ cells at multiple time points post PD-1 blockade. (*C*) Comparison of percent of IFN-γ^+ producing cells as a percent of tetramer$^+$ cells at day 7 post PD-1 blockade. (*D*) Temporal frequency of SIV-Gag-specific IFN-γ^+ CD8 T cells in the blood. (*E*) Temporal frequency of SIV-Gag-specific IFN-γ^+TNF-α^+ CD8 T cells in the blood. (*F*) Temporal frequency of SIV-Gag-specific IFN-γ^+ CD4 T cells in the blood. (*G*) Temporal frequency of SIV-Gag-specific IFN-γ^+TNF-α^+ CD4 T cells in the blood.

Toward this, the therapeutic potential of PD-1 blockade can be further improved by combining it with other therapies such as therapeutic vaccination that can induce strong and broad antiviral CD8 and CD4 T-cell response during ART. It would be important to test the therapeutic benefit of PD-1 blockade in both Mamu-A*01$^+$ and Mamu-A*01$^-$ animals with relatively larger group sizes. In addition, it would be important to test the therapeutic benefit of PD-1 blockade at the time of ART interruption, which would be easier to translate in the clinic.

Materials and Methods

Study Group Animals. Indian adult rhesus macaques were housed at the Emory National Primate Research Center and were cared for under guidelines established by the Animal Welfare Act and the NIH *Guide for the Care and Use of Laboratory Animals* using protocols approved by the Emory University Institutional Animal Care and Use Committee. Eleven Indian rhesus macaques infected with SIV were studied. Seven macaques were used for PD-1 treatment and four were used for the control group. All macaques that were used for the study were infected intravenously with 200 TCID50 of SIVmac251. All macaques were negative for Mamu B08 and Mamu B17 alleles.

In Vivo PD-1 Antibody Treatment. Macaques were infused with 25 mL of Humanized anti–PD-1 Ab (clone EH12 2048) in saline or 25 mL of saline alone for control animals. Anti–PD-1 Ab was administered intravenously at 3 mg/kg of body weight on days 0, 3, 7, 14, 21, and 28 starting 4 wk post ATI. The anti–PD-1 monoclonal Ab (mAb) is derived from the mouse anti–human EH12 mAb (1) and has a humanized variable heavy chain domain linked to a human immunoglobulin G4

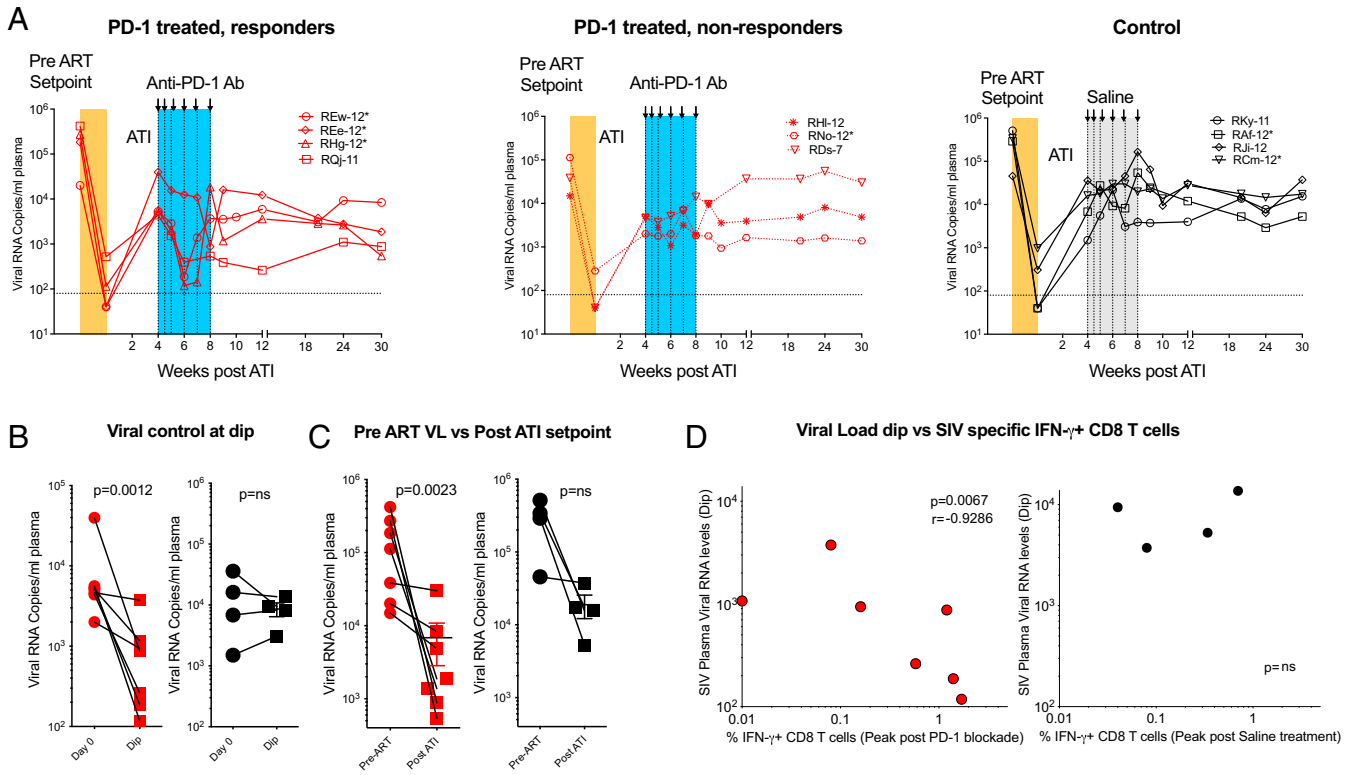

Fig. 4. PD-1 blockade post ATI enhances SIV control. (*A*) Plasma SIV RNA viral levels post ATI for individual animals and after initiation of anti–PD-1 Ab or saline infusion. Limit of detection is 80 copies/mL indicated with a dotted horizontal line. (*B*) Comparison of plasma SIV RNA for individual RMs preblockade time point (week 4 post ATI) and dip (lowest measure between weeks 4 and 8 post ATI) post PD-1 blockade. (*C*) Comparison of set-point plasma SIV RNA levels (copies/mL) pre-ART and post ATI (week 30). (*D*) Association between SIV-specific IFN-γ^+ CD8 T cells at peak post PD-1 blockade with SIV viral RNA levels at the dip in PD-1-treated animals and control animals.

and a humanized variable light chain domain linked to a human kappa. The EH12 mAb binds to RM PD-1 and blocks interaction between PD-1 and its ligands in vitro. Ab was produced in CHO cells using DHFR amplification, purified from culture supernatants by Protein G affinity chromatography, and verified to have an endotoxin level less than 2 EU/mg.

ART Therapy. ART was initiated with the following combination of drugs: azidothymidine (AZT; 5 mg/kg, twice daily), tenofovir (PMPA; 20 mg/kg, daily), emtricitabine (FTC; 30 mg/kg, daily) administered subcutaneously, and Kaletra (12 + 3 mg/kg, twice daily) administered orally (8).

Antibodies. Cells were stained with fluorochrome-conjugated Abs specific for CD3 (clone SP-34-2), CD4 (clone L200), CD8 (clone SK1), PD-1 (Clone EH12.2H7), CD95 (Clone DX2), CD28 (Clone 28.2), K_i-67 (Clone B56), CCR7 (clone 3D1), IL-7R (Clone eBioRDR5), Granzyme B (Clone GB11), Perforin (Clone Pf-80/164), Gag-CM9 tetramer (NIH tetramer core), IFN-γ (Clone B27), TNF-α (MAb11), and LIVE/DEAD fixable Near-IR Dead Cell stain (Invitrogen).

Phenotyping. Mononuclear cells were isolated from the blood and rectum as previously described (1, 8). Mononuclear cells were stained with LIVE/DEAD Near-IR Dead Cell stain (Life Technologies) and samples were acquired on an LSR-Fortessa (BD Biosciences). Cells stained for T-cell phenotyping were stained for surface markers as described above and then fixed and permeabilized with BD perm 2 buffer for staining intracellular antigens as as previously described (15, 16).

Intracellular Cytokine Stimulation and Staining. Mononuclear cells isolated from the blood were stimulated with SIV Gag and P11C peptides, stained and acquired on an LSR-Fortessa, and analyzed using FlowJo software (Tree Star) as previously described (15).

Viral Quantification. The SIV copy number in the plasma was determined by using quantitative real-time PCR as previously described (15).

Titers of Anti-PD-1 Antibody and Monkey Antibody Response against Anti-PD-1 Antibody in Serum. These antibody titers were measured as described previously (16).

Statistical Analyses. A paired *t* test was used for comparisons between two or more subsets from the same animal. Unpaired *t* test was used for comparisons between PD-1-treated and Control antibody-treated animals. Spearman rank test was used for all correlations. The GraphPad Prism statistical analysis program (GraphPad Software 9.0) was used to determine *P* values. *P* values of less than 0.05 were considered significant.

Data Availability. All study data are included in the article and/or *SI Appendix*.

ACKNOWLEDGMENTS. We thank the veterinary staff at Emory National Primate Research Center (ENPRC) for animal care, CFAR virology core for viral RNA, CFAR immunology core for help with flow cytometry, and NIH AIDS Research and Reference Reagent Program for the provision of peptides. This work was supported by the NIH (R37AI112787 to R.R.A., P01AI056299 to G.J.F.), the NIH Office of Research Infrastructure Programs (P51 OD011132 to ENPRC), and Emory CFAR (P30 AI050409).

Author affiliations: [a]Division of Microbiology and Immunology, Emory Vaccine Center, Emory National Primate Research Center, Emory University, Atlanta, GA 30329; [b]Department of Pathology and Laboratory Medicine, Emory University School of Medicine, Atlanta, GA 30322; [c]Department of Microbiology and Immunology, Emory University School of Medicine, Atlanta, GA 30322; [d]Department of Medical Oncology, Dana-Farber Cancer Institute, Boston, MA 02115; and [e]Department of Medicine, Harvard Medical School, Boston, MA 02115

1. V. Velu *et al.*, Enhancing SIV-specific immunity in vivo by PD-1 blockade. *Nature* **458**, 206–210 (2009).
2. C. Petrovas *et al.*, PD-1 is a regulator of virus-specific CD8+ T cell survival in HIV infection. *J. Exp. Med.* **203**, 2281–2292 (2006).
3. C. L. Day *et al.*, PD-1 expression on HIV-specific T cells is associated with T-cell exhaustion and disease progression. *Nature* **443**, 350–354 (2006).
4. L. Trautmann *et al.*, Upregulation of PD-1 expression on HIV-specific CD8+ T cells leads to reversible immune dysfunction. *Nat. Med.* **12**, 1198–1202 (2006).

5. D. L. Barber *et al.*, Restoring function in exhausted CD8 T cells during chronic viral infection. *Nature* **439**, 682–687 (2006).
6. R. Dyavar Shetty *et al.*, PD-1 blockade during chronic SIV infection reduces hyperimmune activation and microbial translocation in rhesus macaques. *J. Clin. Invest.* **122**, 1712–1716 (2012).
7. K. Titanji *et al.*, Acute depletion of activated memory B cells involves the PD-1 pathway in rapidly progressing SIV-infected macaques. *J. Clin. Invest.* **120**, 3878–3890 (2010).
8. G. H. Mylvaganam *et al.*, Combination anti-PD-1 and antiretroviral therapy provides therapeutic benefit against SIV. *JCI Insight* **3**, e122940 (2018).
9. S. A. Rahman *et al.*, PD-1 blockade and vaccination provide therapeutic benefit against SIV by inducing broad and functional $CD8^+$ T cells in lymphoid tissue. *Sci. Immunol.* **6**, eabh3034 (2021).
10. D. H. Barouch *et al.*, Eventual AIDS vaccine failure in a rhesus monkey by viral escape from cytotoxic T lymphocytes. *Nature* **415**, 335–339 (2002).
11. C. M. Walker, D. J. Moody, D. P. Stites, J. A. Levy, CD8+ lymphocytes can control HIV infection in vitro by suppressing virus replication. *Science* **234**, 1563–1566 (1986).
12. A. J. McMichael *et al.*, Memory CD8+ T cells in HIV infection. *Philos. Trans. R. Soc. Lond. B Biol. Sci.* **355**, 363–367 (2000).
13. E. K. Cartwright *et al.*, CD8(+) lymphocytes are required for maintaining viral suppression in SIV-infected macaques treated with short-term antiretroviral therapy. *Immunity* **45**, 656–668 (2016).
14. J. B. McBrien, N. A. Kumar, G. Silvestri, Mechanisms of $CD8^+$ T cell-mediated suppression of HIV/SIV replication. *Eur. J. Immunol.* **48**, 898–914 (2018).
15. R. R. Amara *et al.*, Control of a mucosal challenge and prevention of AIDS by a multiprotein DNA/MVA vaccine. *Science* **292**, 69–74 (2001).
16. V. Velu *et al.*, Induction of Th1-biased T follicular helper (Tfh) cells in lymphoid tissues during chronic simian immunodeficiency virus infection defines functionally distinct germinal center Tfh cells. *J. Immunol.* **197**, 1832–1842 (2016).